Effect of shear connectors on the behavior of composite beams in the linear and nonlinear phases

O. M. Baalbaki
Civil Eng. Department, Beirut Arab University, Beirut, P. O. Box 11-5020, Lebanon
Email:ousabaki@hotmail.com

The aim of the present research is to define a simplified approach which allow the determination of the composite beam behavior; i.e. load capacity versus deflection, based on shear connector properties. Composite beams are widely used in construction, especially for rehabilitation or when seismic effects are to be considered in structural analysis. An advantage feature is that it involves an interaction between structural elements made of same or different structural materials. This leads to an increase in stiffness in addition to structural and economical benefits. A computer program was developed to predict the behavior of composite beams under flexure in the linear and non-linear phases. Many researchers have dealt with the effect of partial composite action in the elastic zone. However, few studies have revealed the nonlinear response of composite beams with regard to the behavior of shear connectors. In the present work, a new approach using discretization method was presented for the implementation of the composite effect for nonlinear analysis purpose. An experimental program was established on a series of composite beams with different shear connector characteristics. Based on shear connector characteristics, full or partial action is to be considered. The validity of this approach was established by correlation of numerical results with experimental test evidence.

إن الغرض من هذا البحث هو إيجاد طريقة مبسطة تسمح بتحديد تصرف الكمرة المركبة (علاقة الهبوط بالحمل) على أساس خصائص روابط القص. يعتبر استخدام الكمرات المركبة شائعاً في مجال الإنشاءات خصوصاً لتأهيلها ولزيادة قدرتها على مقاومة الزلازل. تتكون الكمرات المركبة من قطاعات مصنوعة من نفس المواد أو مواد إنشائية مختلفة تترابط مع بعضها البعض مما يؤثر في زيادة صلابتها وقدرة تحملها للأحمال. ولذلك فوائد من الناحية الإنشائية والاقتصادية. لقد تم تطوير برنامج كومبيوتر يمكن من خلاله توقع تصرف الكمرات المركبة عند تعرضها للإنحناء في المرحلة المرنة وغير المرنة. هنالك عدد من الدراسات التى ركزت على موضوع التأثير النسبي للروابط في المرحلة المرنة. أما فى المرحلة الغير مرنة، فالقليل من الدراسات تناولت الموضوع آخذة في الإعتبار تصرف الروابط نفسها. تعتمد هذه الدراسات على طريقة التجزئة العددية لدراسة تأثير الترابط في المرحلة الغير مرنة بهدف أخذها في الأعتبار في التحليل والتصميم. كما تم وضع برنامج تجارب عملية على مجموعة من الكمرات المركبة بإستخدام روابط ذات خصائص مختلفة. بناء على صلابة الروابط والمسافة بينها يتغير تصرف الكمرة حسب نسبة الترابط حيث تتراوح بين الترابط الكلي والجزئي. إن مطابقة النتائج العددية مع التجارب العملية تعزز صلاحية الطريقة المستخدمة .

Keywords: Shear connectors, Shear interface, Composite action, Composite beam, Elastic behavior, Nonlinear behavior

1. Introduction

The stiffening and strengthening of beams using composite construction materials is a suitable technique, which appears particularly for restoration as well as for increasing the resistance against lateral forces [1]. The objective of this research is to study the role of shear interface on the composite effect. The composite beams such as steel beam and concrete slab are widely used as structural materials due to their ability to absorb dynamic loads. The use of such system allows reduced beam depth and increased stiffness. Thus, it can be more economical at longer span.

The studs (shear connectors) comprise the most basic element of the system creating a “link” between the upper part and the lower part element. This allows them to work together to support the load. Composite construction as treated in this paper consists of steel plate placed upon and interconnected to

© Faculty of Engineering Alexandria University, Egypt.

a steel rolled I-section shaped girder. In the United States, the design provisions of composite structural members can be found in the American Concrete Institute building code No. (ACI 318 1999) [2], the American Institute of Steel Construction (AISC 1999) [3], and the National Hazards Earthquake Program (NEHRP) seismic provisions (BSSC 1997) [4].

However, due to lack of sufficient data on shear connector effect, it is noted that the design provisions of composite structural members have not included the partial effect of shear connectors. An experimental study on the mechanical behavior of steel I-section shaped composite beam subjected to bending was conducted on a series of specimens. A computer program was developed for that purpose. The results of the theoretical formulation are in good agreement with experimental data. The importance of this study is that the non-linearity is taken into consideration in the approach. The objectives are to develop a model for predicting the influence of upper plate and bond conditions on the behavior of composite beams and to propose a new approach to evaluate the percentage effect of composite action. Also to study the parameters that increases the stiffness and the load capacity of the composite beam.

2. Composite action

Composite action is developed when two load carrying structural members such as steel plate and the supporting steel beam are integrally connected and deflect as a single unit. Viest notes that the important factor in composite action is the bond between the upper and lower part of the composite beam [5]. The shear connectors provide the interaction necessary for the system to act as a unit; i.e. no slip between the upper and the lower part of the beam. The shear forces are transferred across the interface [6, 7].

In developing the concept of composite behavior, consider first the non-composite behavior where friction is neglected, the beam and plate each carry separately a part of the load. When the plate deforms under vertical load, its lower surface is in tension and elongates, while the upper surface of the beam is in compression and shortens. Thus a discontinuity occurs at the plane of contact. Since friction is neglected, only vertical forces act between the plate and the beam. This is shown in the fig. 1-a. By examination of the strain distribution that occurs when there is no interaction between upper and lower plate as shown in fig. 2-a, it is seen that the total resisting moment is equal to the summation of the plate and beam moments eq. (1-a). There are two neutral axes, one at the center of gravity of the plate and the other at the center of gravity of the I-beam. Horizontal forces (shear forces) are developed on the lower surface of the plate to compress and shorten it, while simultaneously they act on the upper surface of the beam to elongate it; fig. 1-b. When partial interaction is present, the center of gravity of the plate and beam are closer to each other and the slip is decreased as shown in fig. 2-b. The moment is given in eq. (1-b). When a system acts compositely, no relative slip occurs between the plate and the beam. There will be one single neutral axis; fig. 2-c. The moment is then obtained by eq. (1-c).

$$\sum M = Mplate + Mbeam, \quad (1\text{-a})$$

$$\sum M = T'.e' \text{ or } C'.e', \quad (1\text{-b})$$

$$\sum M = T''.e'' \text{ or } C''.e''. \quad (1\text{-c})$$

3. Computer program development

3.1. Elasto-plastic behavior

Computer software was developed to predict the full behavior of the composite member in the elastic and elasto-plastic phases under bending load. The composite member consists of an I-section shaped beam supporting a rectangular plate. In this research, the same material properties were selected for both the beam and plate. We have studied the case of a simple beam supporting a single concentrated load. Knowing that the

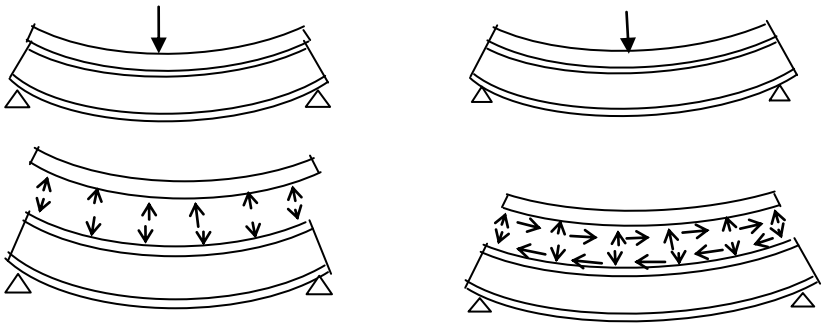

(a) Deflected non-composite beam (b) Deflected composite beam

Fig. 1. Comparison of deflected beam with and without composite action.

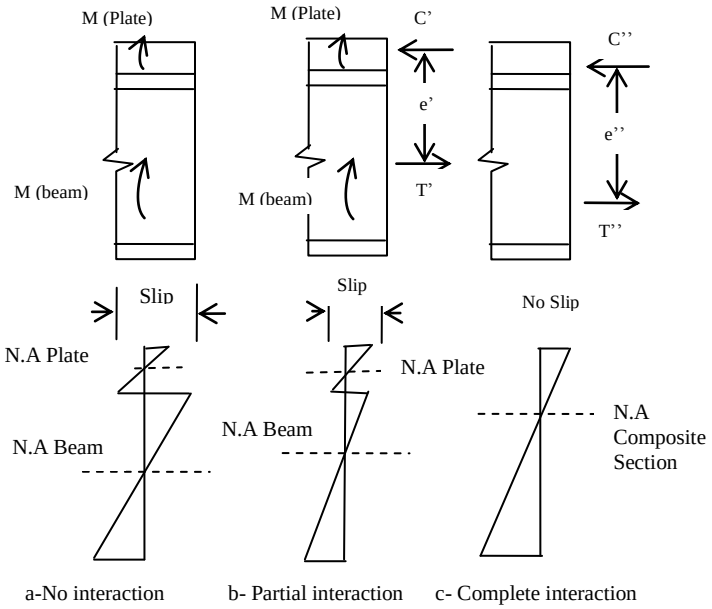

Fig. 2. Strain variation in composite beams [6].

program can be modified to consider the composite member made of two different materials such as steel and concrete of different stiffness. For pure elastic deformation, we assume that Hooke's law applies throughout the member. If the yielding strength is exceeded in some portion of the member, or the material involved is a brittle with a nonlinear stress strain diagram, this relation ceases to be valid.

When designing within the elastic range, the load capacity of the composite member is then computed based on the proportional relationship (2) between the applied load P and the deflection y. Therefore, there is no need for a computer program and the relation will be in case of single load acting on the mid-span of a simply supported beam:

$$y = \frac{PL^3}{48_{\dot{E}I}} \tag{2}$$

where E and I are the modulus of elasticity and the inertia of the section.

While, in case the stresses in the members exceed the elastic proportional stress and enter the elasto-plastic zone, the load capacity will depend on the behavior of the material as well as the size and shape of the composite

member. The position of the neutral axis is also an aspect to be considered. As the load increases, the maximum stresses at the top and bottom increases accordingly up to the yielding stress. Assuming the yielding stress in tension and compression are equal. Therefore, the yielding stress appears first at the bottom where the distance from the neutral axis to the bottom edge is greater than that to the top edge due to the presence of the upper plate in our case. As long as the normal stress does not exceed the yield stress, Hooke's law applies, and the stress distribution across the section is linear as shown in fig. 3-a. The maximum value of the stress is σ_Y in case of an elasto-plastic material. As the bending moment increases σ_X eventually reaches the value σ_Y. As the bending moment further increases, plastic zones develop in the member with the stress uniformly equal to ($-\sigma_Y$) in the upper zone and ($+\sigma_Y$) in the lower zone; fig. 3-b. Between the plastic and elastic zone an elastic core subsists and the stress varies linearly with the following eq. (3):

$$\sigma_X = \frac{\sigma_Y}{y_Y} y , \qquad (3)$$

where y_Y represents a part of thickness of the elastic zone.

We shall use eq. (4) to determine the value of the bending moment (see figs. 3 & 5 for the notations):

$$, M = \int_0^{Cc} b.\sigma.dA.y + \int_0^{Ct} b.\sigma.dA.y \qquad dA=b.dy. \qquad (4)$$

Where for: $0 \le y \le y_Y$ $\quad \sigma_X = \frac{\sigma_Y}{y_Y} y$,

$y_Y \le y \le c$ $\quad \sigma_X = \sigma_Y$.

We note that when y_Y approaches zero, the bending moment approaches the limiting value. This value corresponds to the plastic moment M_p, eq. (5), fig. 3 ©.

$M_p=k.M_y$ where M_y is the moment at start of (5) the yield and k is the shape factor.

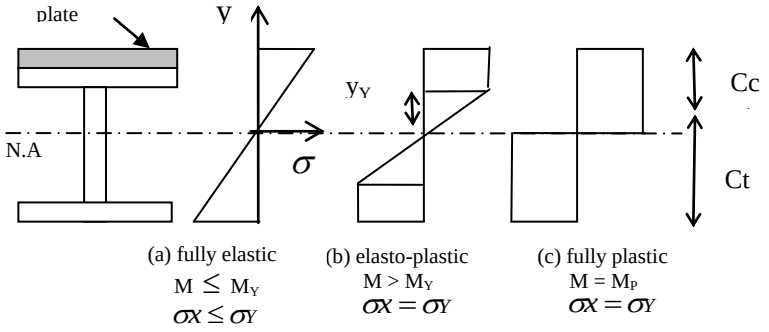

Fig. 3. Stress distribution of an elasto-plastic material (full composite case).

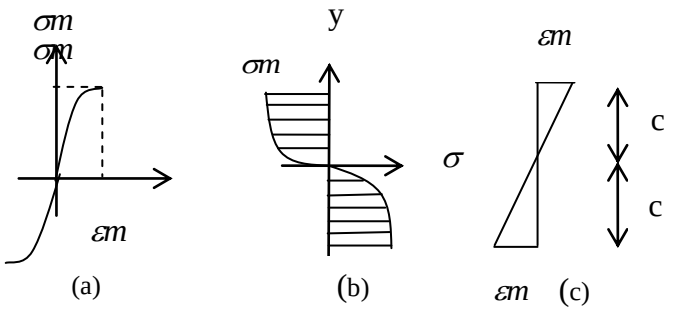

Fig. 4-a. Stress-strain curve, (b) & (c) Stress and Strain distribution over the cross section.

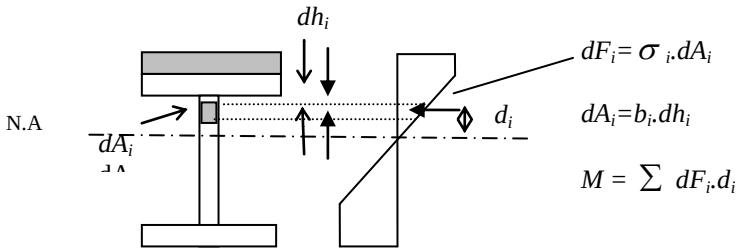

Fig. 5. Discretization of the stress diagram (full composite case).

For rectangular section, the width (b) =constant and k = 1.5. It should be kept in mind that the distribution of strain across the section remains linear after the onset of yield. Therefore eq. (6-a,b) is used:

$$y_Y = \varepsilon_Y \rho \,, \tag{6-a}$$

$$\varepsilon_Y = \frac{\sigma_Y}{E} \,, \tag{6-b}$$

where ρ is the radius of curvature.

For beams of variable cross section, the computation of the plastic moment will usually be simplified if a graphical method of analysis is used.

3.2. Nonlinear behavior

The purpose of this section is to develop a more general method for the determination of the distribution of stresses in a member in pure bending, which may be used when Hooke's law does not apply. We first recall that no specific stress strain curve was assumed. The normal strain εx varies linearly with the distance y from the neutral surface fig. 4 ©. Thus still eqs. (7-a,b):

$$\varepsilon x = \frac{\varepsilon_Y}{y_Y} y \,, \tag{7-a}$$

$$\frac{\varepsilon x}{\varepsilon m} = \frac{y}{c} \,. \tag{7-b}$$

Where y represents the distance from the point considered from the neutral surface, and c is the maximum value of y. A material characterized by the same strain relation in tension and compression, the neutral axis will coincide with the horizontal axis of symmetry of the section. Considering the distribution of the strain is linear and symmetrical with respect to the horizontal axis. The stress strain curve is assumed to be symmetrical with respect to the origin of coordinates.

The distribution of the stresses in the cross section of the member i.e., the plot of σx versus y, is obtained as follows. Assuming that σ_m has been specified. We first determine the corresponding value of εm from the stress strain diagram and carry this value into the eqs. (6,7). Then for each value of y, we determine the corresponding value of εx and obtain from the stress strain diagram the stress corresponding to this value of εx. Plotting σx against y, yields the desired distribution of stresses.

If σx is a known analytical function of εx, then σx can be expressed as function of y and the integral of the moment eq. (4) can be determined analytically. Otherwise, the bending moment may be obtained through a numerical integration. An important value of the bending moment is the ultimate bending moment M_u which causes failure of the member. This value can be obtained from the ultimate strength σu of the material. However, it is found more convenient in practice to determine experimentally M_u for a specimen of a given material.

3.3. Numerical approach

The computation of the moment in the computer program is based on the discretization method. As the bending load increases, the stress distribution diagram is plotted over the cross section. We have selected the mid span section where the deflection is the maximum. The corresponding stress distribution is plotted and divided into

strips for computation of the moment. The total moment is equal to the summation of all strips where each strip has a moment eq. (8-a,b):

$$\Delta M_i = dF_i.d_i.b_{(h)} \,, \tag{8-a}$$

$$M = \sum \Delta M_i \,, \tag{8-b}$$

where: dF_i is the area of the strip, d_i is the distance from the centroid of the strip to the centroid of the composite section, and $b_{(h)}$ is the width of the section at the centroid level of the strip.

The computer program has a subroutine function which allows the determination of the width b at any level of the section. For each load, there will be a corresponding value of the actual moment according to the stress distribution diagram; fig. 5. The load deflection curve is then plotted illustrating the full behavior of the section to be studied. The importance of this program is that it can be integrated into a computer structural analysis program so that each section of the structural element can be checked.

4. Experimental program

4.1. Test set up

The load deformation curve was determined using an automated testing machine provided with data acquisition unit. On line measurements of load and deflection are taken from transducers and transferred to the P.C. through the data acquisition unit. Specialized software allows the on-line monitoring of the load deflection curve. A large number of readings per second can be specified allowing an accurate and smooth transition of the curve. The load is acting monotonically at the mid-length of the specimen through a displacement control method. The load produces single curvature bending in all specimens with bending moment acting about the major axis of the steel shape. The deflection is measured through LVDT while, the load P is monitored from both the gauge of the machine and from the computer; fig. 6.

4.2. Test specimens

In this study, steel I-beams of 1000 mm span length were tested. Table 1 shows the materials and section properties of the test specimens (beams and plates). The material consists of mild steel, which shows high ductility under testing. The yielding stress f_y and the ultimate tensile strength f_u of steel shape are determined according to ASTM method of universal tension testing of metallic materials (E8-91); [8]. Before conducting the load deflection test, the materials properties were determined. The results shown in the table represent the range of all materials data obtained. The composite girders consist of an I-beam supporting a rectangular plate of different thicknesses. The connection of the plate with the beam is ensured through the shear connectors. Tests were conducted using shear connectors of different stiffness and spacing.

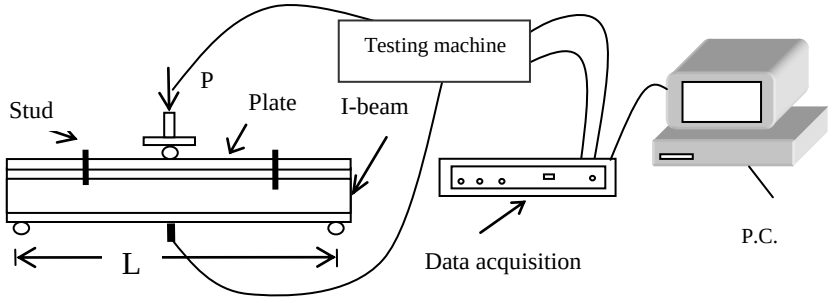

Fig. 6. Test set up system.

Table 1
Materials and section properties

Section properties		Mechanical characteristics	
I- Beam			
Designation:	IPE 100	Modulus of elasticity:	E = 130 – 150 MPa
Total height:	h=100 mm	Yield Stress:	f_y = 250 – 300 MPa
Web thickness:	b_w=4.1 mm	Ultimate Stress:	fu = 300 – 350 MPa
Flange width:	b_f=55 mm		
Cross section area:	A = 10.3 x 10^2 mm^2		
Inertia:	I =1.6332 x 10^6 mm^4		
Plates			
Designation:	*Pl* 10 & Pl 20		
Dimensions:	*Pl10* :10 x 50 mm		
	*Pl*20: 20 x 50 mm		

5. Test results and discussions

5.1. Validation of the discretization method

The validation of the program was checked by comparison of experimental test results with numerical data obtained from the program. The figs. 7 and 8 compare between the load deformation curves obtained from experiments conducted on specimens and that obtained from numerical analysis based on actual materials properties and dimensions. This shows the conformity of test results and the validity of the approach. Two cases were studied. A full composite action was ensured by welding the plate and the beam from all sides. For non-composite action case, the plates were supported by the I-beam without any connection. It is shown that when the stress exceeds the maximum proportional limit, the behavior does not become fully plastic. This is indicated by the slope of the load deflection curve after the elastic zone. Therefore, due to strain hardening, there is no pure plasticity as it is theoretically assumed when calculating the plastic moment; fig. 9 (b). The program calculates first the fictitious moment based on the fictitious stress (elastic stress) and then makes correction based on the actual maximum stress; fig. 9 (a) which exceeds the yielding stress. The actual moment as well as the actual maximum stress are smaller than the fictitious moment and the corresponding stress; fig 9 (c). The decrease in moment is then equal:

$$\Delta M = M_{fictitious} - M_{actual} . \quad (9)$$

The load deformation curve is plotted for full composite and non-composite action considering the actual materials strength. The role of shear interface appears when comparing the load deformation curve of full and non-composite action [9,10]. The increase in the load capacity as demonstrated in fig. 7 is due to the effect of shear connection. As the thickness of the plate increases, the inertia of the assembly as well as the load capacity is amplified; fig. 10.

6. Shape factor

The influence of beam section shape on the load capacity curve was studied using the program. The I-beam section shape was replaced by a rectangular shape. The inertia of the system was kept constant. The equivalent width (b) was calculated accordingly to provide the same inertia of the system. The fig. 11 indicates that the load capacity was increased only in the non-elastic case in case of rectangular shaped beam due to the larger cross sectional area. A shape factor can be deduced for each shape cases based on a standard shape.

6.1. Effect of shear connectors

The horizontal shear that develops between the plate and the I-beam during loading must be resisted so that the slip at the interface will be restrained. It is evident that the composite action depends on the properties of shear connectors [11-13]. In order to study the effect of shear connectors,

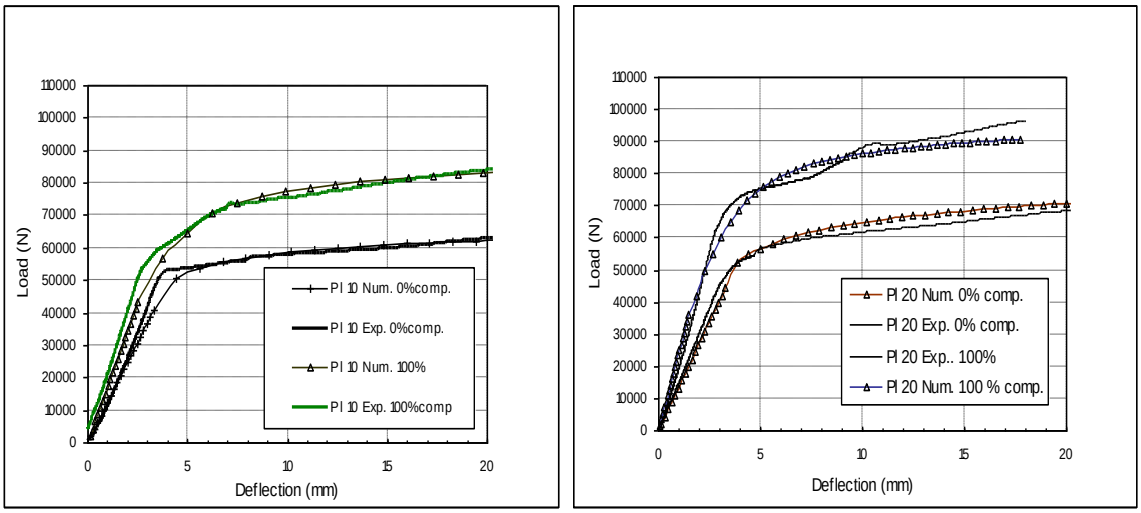

Fig. 7. Experimental and Numerical comparison of load-deflection curves using Pl 10 & Pl 20.

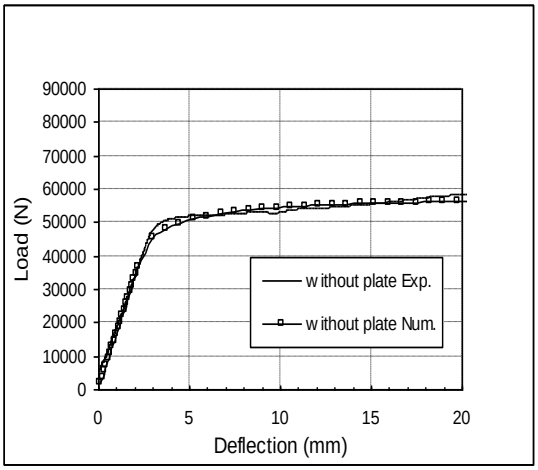

Fig. 8. Load-deflection curves without upper plate.

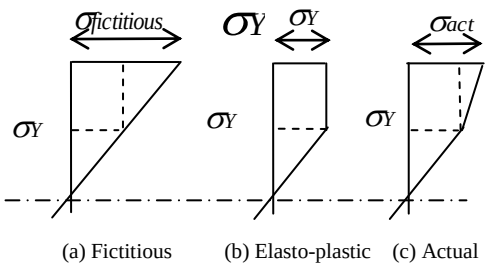

Fig. 9. Stress distribution diagrams.

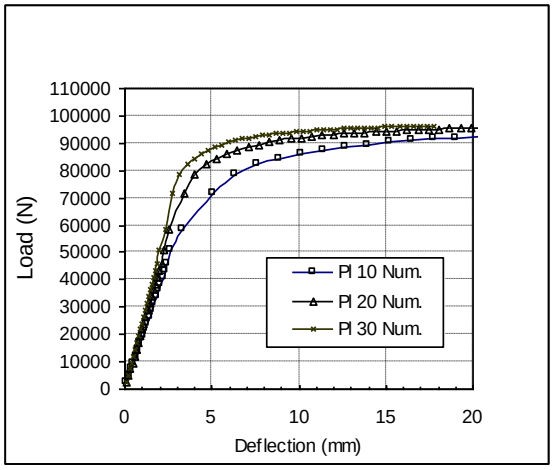

Fig. 10. Load-deflection curves (Pl 10-20-30, Num.).

its behavior has to be determined through shear test [14,15]. A section of the beam is attached to plates (Pl 10) on both sides as shown fig. 12. The load applied on the cross section is distributed on four bolts. The load displacement per each bolt is plotted illustrating the behavior of the stud; fig. 13. Two types of stud were studied of high and low stiffness. The stiffness factor S_t of the bolt is calculated from the slope of the initial portion of the curve.

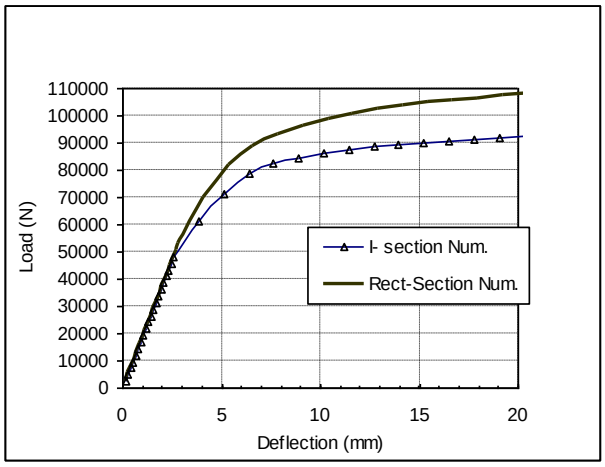

Fig. 11. Load-deflection of I and rect. section shaped beam (Pl 10, beq=15.5 mm, Isys=26438x10^6 mm^4).

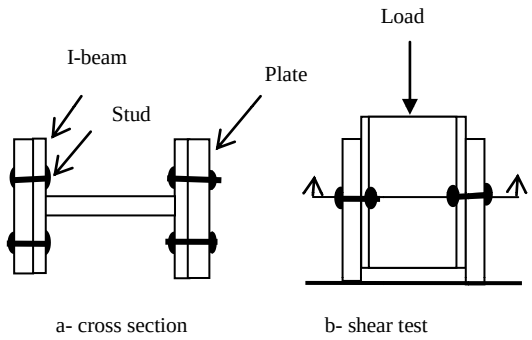

Fig. 12. Shear connector test.

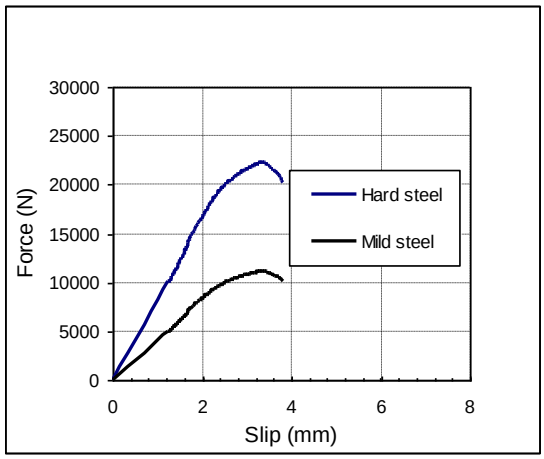

Fig. 13. Behavior of shear connectors (high and low stud stiffness).

6.2. Partial composite action

The connection stiffness evaluation is important because the composite beam deflection is strongly influenced by the slip between the beam and plate. Taking full advantages of composite system, this permits the use of shallower depth as well as lighter member. This advantage may increase the span length and reduce the height of multistory buildings materials such as outside walls and stairways. The suggested approach is based on the fact that, for partial composite action the load-deflection curve should be situated between the two curves representing the fully composite and the non-composite action cases. The program is able to compute the shearing force F per each shear connector due to the bending load at the shear interface level as follows:

$$\tau = \frac{V.\eta}{Isys}, \qquad (10\text{-a})$$

$$F = \tau.S, \qquad (10\text{-b})$$

$$S = \frac{L}{N}. \qquad (10\text{-c})$$

Where; τ is the shearing stress, V is the shearing force at the section, I_{sys} is the inertia of the system, η is the moment of area of the plate about the center of gravity of the assembly, F is the force per each stud, S is the spacing between connectors, L is the span length and N is number of rows (two studs per row were used).

Also, the program computes the shearing strain/deformation (δ_{int}) assuming a full composite action at the interface level. The shearing force versus deformation curve at the interface can be plotted and compared to the stiffness stud curve; fig. 14. The shear force-slip curve is relative to the cross section dimension of beam and plates used. For each shearing force, there will be a corresponding shearing strain/deformation in the interface. This will be compared to the actual shearing strain/deformation occurred in the stud (δ_{stud}). The composite action factor is then calculated as follows:

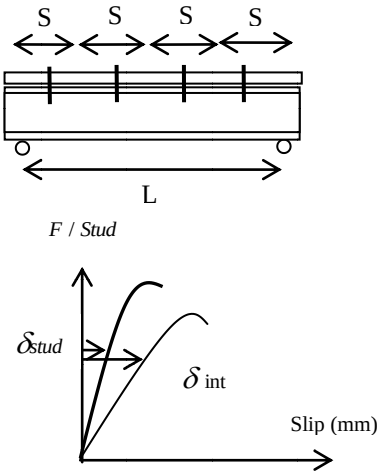

Fig. 14. Shear interface and stiffness stud curves (shearforce – slip).

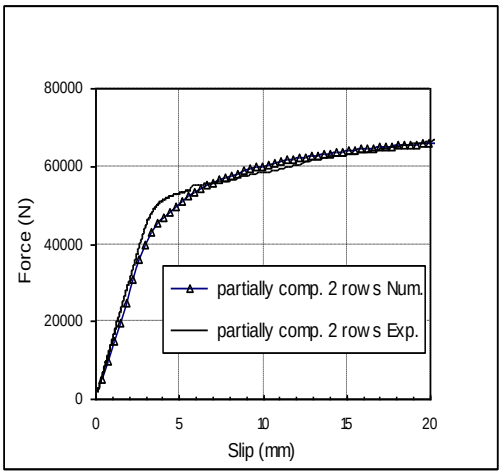

(a)

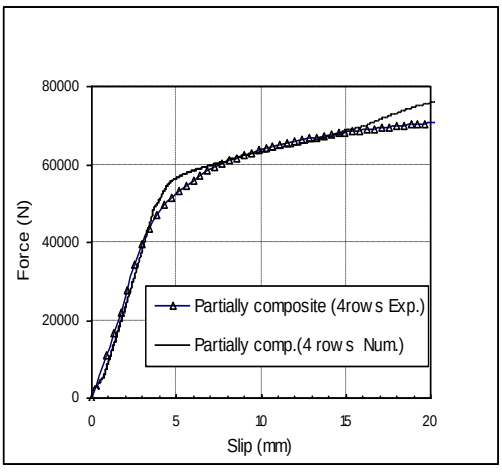

(b)

Fig. 15. Comparison of load deflection curve for partial composite action (a: 2 rows & b: 4 rows)

$$k = \frac{\delta_{int} - \delta_{stud}}{\delta_{int}} \quad . \qquad (11)$$

There are three cases:
- $k \leq 0 \Rightarrow$ stiffness factor of stud is lower than that of interface $\Rightarrow$ No composite action,
- $k > 0 \Rightarrow$ stiffness factor of stud is greater than that of interface $\Rightarrow$ Partial composite action,
- As k increases $\Rightarrow$ this leads to fully composite action.

The load capacity for partial composite action case is then equal to the load capacity in case of non-composite action plus the difference between the load corresponding to the fully composite and non-composite action computed from the program and multiplied by the composite factor action; eq. (12). Fig. 15 shows that our approach for the computation of the percentage of composite action is reasonable. Experimental results are illustrated in the same graph indicating that partially composite action curves are situated between the non-composite and fully composite curves; fig. 16.

$$P_{partial} = P_{non\text{-}comp} + (P_{fully\ comp.} - P_{non\text{-}comp}).\ k. \qquad (12)$$

6.3. Influence of stud stiffness

Using other type of studs made of mild steel where the stiffness is reduced to the half, the experimental results shown in the fig. 17 confirm that the stiffness of studs has an essential role in the composite action. It is shown that even when the number of rows is increased, there will be no composite action. It is evident that the composite action factor depends on the stiffness factor which reflects the behavior of the stud. The numerical results for different stiffness values are illustrated in fig. 18.

6.4. Influence of stud spacing

It is known that as the spacing between studs decreases, the shearing force per each stud increases. This will help in increasing the composite action which affects the load deflection curve as it is indicated in the numerical results shown in fig. 19. The spacing factor S_p has to be taken into consideration in

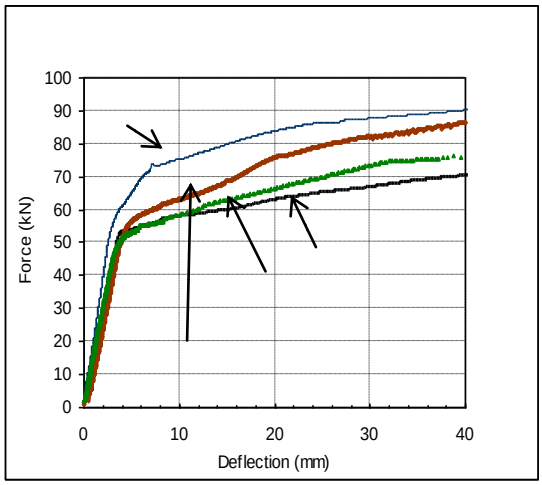

Fig.16. Exp. tests (Hard steel stud & Pl 10).

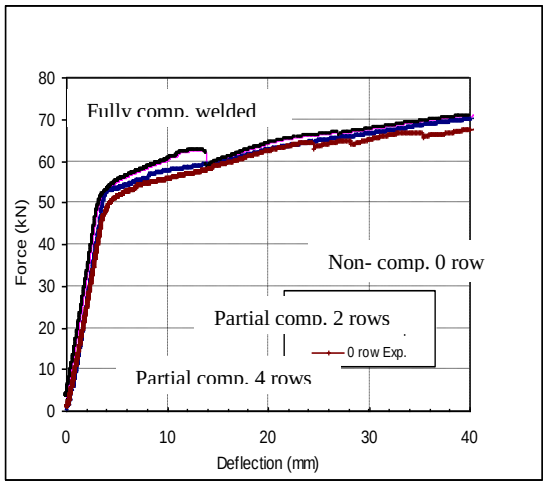

Fig. 17. Exp. Results (Mild steel stud & Pl 10).

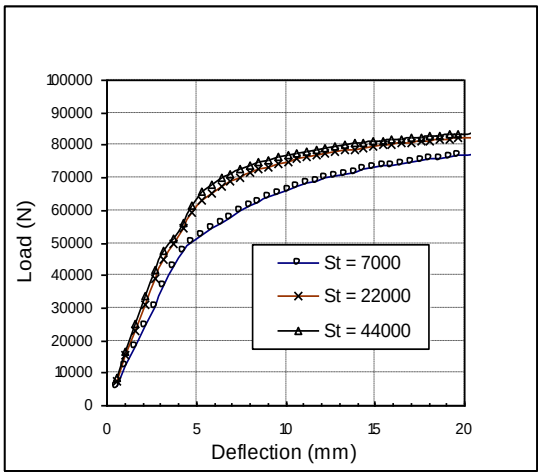

Fig. 18. Effect of stiffness on the load deflection (Pl 10).

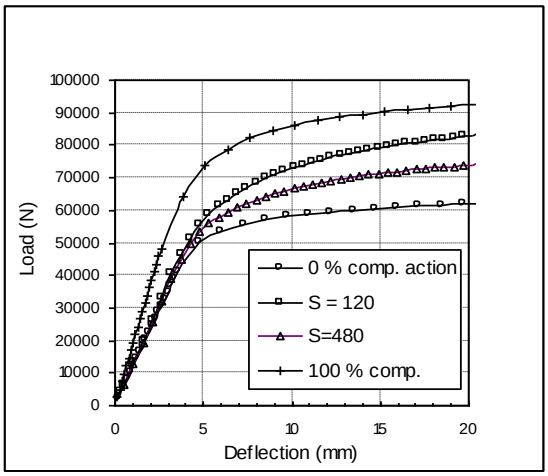

Fig. 19. Effect of spacing on the load deflection (Pl 10).

the calculation of the composite factor; eq. (13). Where, for a theoretical spacing equal to span length, the spacing factor equal zero.

$$K_{corrected} = k.S_p = k.\frac{L-S}{S}. \qquad (13)$$

7. Conclusions

The overall economy of using composite construction when considering total building cost appears to be increasingly favorable. The rehabilitation requires stiffening works to enhance structural performance. The widely adopted technique of composite beams allows an increase in stiffness and load capacity. A particular care must be paid to the connection design concerning stud stiffness and spacing to ensure a perfect composite action. To obtain a fully composite action, the shear connectors should be stiff enough to provide complete interaction. For partial composite action, the load deflection curve falls between that of fully composite and non composite cases. The computation of the load capacity of composite beam is performed by a computer program, based on the actual stress distribution over the section and using the discretization method. The percentage of composite action is obtained based on shear connectors stiffness and spacing parameters. Assuming full composite action, the nominal strength of the section greatly exceeds the sum of the strengths of the plate and the beam consid-

ered separately, providing high overload capacity. The proposed method gives satisfactory predictions as compared to the test results.

References

[1] M. Wakabayashi, "A historical study of Research on Composite Construction in Steel and Concrete in Japan.", Proc. Conf. Composite Construction in Steel and Concrete, ASCE, New York, pp. 400-427 (1987).

[2] Building code requirements for structural concrete (ACI 318-99) and commentary (ACI-318R-99) ACI 318-99, Farmington Hills, Mich (1999).

[3] "Load and Resisting Factor Design Specification for Structural Steel Buildings." American Institute of Steel Construction, AISC, Chicago (1999).

[4] NEHRP recommended provisions for the development of seismic regulations for new building and other Structures National Earthquake Hazards Reduction Program, Building Seismic Safety Council, (BSSC) Washington, D.C. (1997).

[5] I.M. Viest, J.P. Colaco, and R.W. Furlong, Composite Construction Design for Buildings, McGraw-Hill, New York (1997).

[6] R.M. Lawson and K.F. Chung, Composite Beam Design to Eurocode 4, The Steel Construction Institute, Ascot (1994).

[7] A. Ayoub and F.C. Filippou, "Mixed Formulation of Non-linear Steel-Concrete Composite Beam Element", Journal of Structural Engineering, March, pp 371-381 (2002).

[8] ASTM (1991b), Standard methods for tension testing of metallic materials ASTM, E8-91, Philadelphia (1991).

[9] C.W. Roeder, R. Chmielowski, and C.B. Brown "Shear Connector Requirements for Embedded Steel Sections," Journal of Structural Engineering. 125 (2), pp. 142-151 (1999).

[10] M.R. Salari, E. Spacone, AND P.B. Shing, "Nonlinear Analysis of Composite Beams With Deformable Shear Connectors", J. of Structure and Engineering, ASCE, Vol. 124 (10), 1148-1158 (1998).

[11] C.C. Weng, S. I. Yen, and M.H. Jiang, " Experimental Study on Shear Splitting of Full-Scale Composite Concrete Encased Steel Beam", Journal of Structural Engineering, September, pp 1186-1194 (2002).

[12] P. Gelfi, E. Giuriani and A. Marini. "Stud Shear Connection Design for Composite Concrete Slab and Wood Beams", Journal of Structural Engineering, December, pp 1544-1550 (2002).

[13] P. Gelfi, E. Giuriani and A. Marini, "Behavior of Stud Connectors in Wood Concrete Composite Beams," Proc. Structural Studies, Repair and Maintenance of Historical Buildings, VI 6th International Conf., Germany, pp 565-578 (1999).

[14] American Society for Testing and Materials (ASTM), Standard test method for evaluating dowel-bearing strength of wood based products, STD-ASTM 5764-97a (1997).

[15] L. Biolzi and B. Guiriani, "Bearing Capacity of a Bar Under Transversal Load", Materials and structures (23), pp 449-456 (1990).

Received September 4, 2003
Accepted November 30, 2003